Planet. Space Sci., Vol. 40, No. 5, pp. 595–606, 1992
Printed in Great Britain.

0032-0633/92 $5.00 + 0.00
Pergamon Press Ltd

HOW THE EFFECTS OF WINDS AND ELECTRIC FIELDS IN F2-LAYER STORMS VARY WITH LATITUDE AND LONGITUDE: A THEORETICAL STUDY

M. MENDILLO and X.-Q. HE
Center for Space Physics, Boston University, Boston, MA 02215, U.S.A.

and

H. RISHBETH
Physics Department, University of Southampton, Southampton SO9 5NH, U.K.

(*Received* 11 *December* 1991)

Abstract—The effects of thermospheric winds and electric fields on the ionospheric F2-layer are controlled by the geometry of the magnetic field, and so vary with latitude and longitude. We adopt a simple model of the daytime F2-layer and study the effects at midlatitudes (25°–65° geographic) of three processes that accompany geomagnetic storms: (i) thermospheric changes due to auroral heating; (ii) equatorward winds that tend to cancel the quiet-day poleward winds; and (iii) the penetration of magnetospheric electric fields. At ±65°, the effects of heating and electric fields are strongest in the longitudes towards which the geomagnetic dipole is tilted, i.e. the North American and the South Indian Ocean sectors. Because of the proximity of the geomagnetic equator to the East Asian and South American sectors, the reverse is true at ±25°.

1. INTRODUCTION

Thermospheric winds and electric fields are known to play important roles in the complex phenomena of F-layer storms. This is particularly so in the initial stages of storms, when magnetospheric electric fields penetrate to middle and low latitudes, and heating in the auroral oval drives strong equatorward winds. In this paper we show, from simple theoretical calculations using a steady-state model of the F2-layer, that the effects of both winds and electric fields vary markedly with longitude as well as latitude. We find that electric field effects are pronounced in certain longitude sectors, while wind effects predominate in others. However, we do not include the major wind-induced composition changes that cause electron depletions ("negative storm effects") in the main phase of F-layer negative storms (e.g. Duncan, 1969; Prölss, 1980; Rishbeth, 1991). Our calculations therefore apply mainly to the early stages of storms, when electric field effects are pronounced, but before the composition changes become dominant. Even with our simple model, the F2-layer effects vary geographically in quite complicated ways, and our results may be helpful in interpreting the behaviour of the real F2-layer.

2. CALCULATIONS

All the calculations are carried out for equinox at 15:00 L.T., a local time when the F2-layer is generally in a stable state and conditions are relatively simple, and for a moderate level of solar activity (10.7 cm flux = 120 units). In the absence of vertical drift, the F2-layer is taken to be in a steady state under the action of solar photoionization, chemical loss and plasma diffusion. The F2 peak is then at the "balance height" h_bF2. We then assume that a vertical drift velocity W is imposed on the layer by winds and electric fields, adopting very simple time-independent formulas in order to demonstrate clearly how the magnetic field geometry—in particular, the magnetic declination D and the dip (or inclination) I—controls the F2-layer effects. Plasma diffusion is also influenced by the magnetic field geometry, because of the $\sin^2 I$ factor in the coefficient for diffusion in the vertical direction.

An electric field **E**, positive in the geomagnetic eastward direction and normal to the geomagnetic field **B**, produces a vertical plasma drift

$$W_E = (E/B)\cos I. \tag{1}$$

Assuming the ionospheric electric field to be produced by a dawn–dusk electric field in the magnetosphere, we take W_E to vary with magnetic dipole latitude Λ according to the formula of Lanzerotti *et al.* (1975) which, cast in our notation, is

$$W_E = -\left(\frac{E_{DD}}{B_0}\right)\left(1+\frac{h}{R_E}\right)^3 \cos\left(\frac{\pi t}{12}\right)\frac{\sec^2\Lambda}{(1+3\sin^2\Lambda)} \tag{2}$$

which, using the dipole field identity

$$\cos I = \frac{\cos \Lambda}{(1+3\sin^2 \Lambda)^{1/2}} \tag{3}$$

becomes

$$W_E = -\left(\frac{E_{DD}}{B_0}\right)\left(1+\frac{h}{R_E}\right)^3 \cos\left(\frac{\pi t}{12}\right) \times \cos I \sec^3 \Lambda (1+3\sin^2 \Lambda)^{-1/2} \tag{4}$$

where E_{DD} is the magnetospheric dawn–dusk electric field in the equatorial plane, h is height, t is local time, R_E is the Earth's radius and B_0 is the magnetic flux density at the ground at the geomagnetic equator. This formula assumes that the dawn–dusk electric field is spatially uniform in the equatorial plane of the magnetosphere. Although this assumption is oversimplified (and causes difficulty at high magnetic latitudes, where sec Λ becomes large), it enables us to isolate the effects of the penetration electric field from other factors.

Theoretical studies have shown that shielding of the daytime midlatitude ionosphere from a suddenly imposed magnetospheric electric field requires a few hours (Jaggi and Wolf, 1973; Southwood, 1977). Recent convection studies (Spiro *et al.*, 1988; Fejer *et al.*, 1990) show penetration durations of about 1 h. The daytime response modelled in our paper is consistent with observations of electrodynamic storm effects within an hour of onset in the afternoon sector (Evans, 1973).

We take the quiet-day winds from the empirical model of Hedin *et al.* (1988). Although this model does contain longitude variations, our initial calculations use longitude-averaged (though latitude-dependent) wind velocities, in order to isolate the effects of the magnetic field geometry. The vertical plasma drift due to a horizontal wind of speed U blowing at geographic azimuth Ψ is (e.g. Rishbeth, 1972)

$$W_W = -U\cos(\Psi - D)\cos I \sin I. \tag{5}$$

Writing $U_N = U\cos\Psi$ for the south-to-north component and $U_E = U\sin\Psi$ for the west-to-east component of U, (5) becomes

$$W_W = -(U_N \cos D + U_E \sin D)\cos I \sin I. \tag{6}$$

For the chosen conditions of 15:00 L.T. at equinox, the quiet-day wind blows approximately towards the geographic pole (see Fig. 5 of Rishbeth, 1972), i.e. $\Psi = 0°$ in the Northern Hemisphere (I positive) and $\Psi = 180°$ in the Southern (I negative), so that W_W is negative (i.e. downwards) in both hemispheres.

We adopt the F2-layer "servo model" in the form used by Rishbeth *et al.* (1978) (RGW), using RGW equation (12) for steady state (i.e. with $dz_m/dt = 0$) to compute the change of height Δh_m of the F2 peak caused by the vertical plasma drift W. This drift moves the peak from its undisturbed "balance" height h_bF2 to its "perturbed" level $h_WF2 = h_bF2 + \Delta h_m$. The MSIS-86 model of Hedin (1987) is used to convert between z_mF2 (the "reduced height" of the peak, measured in units of scale height) and h_mF2 (the real height in kilometers). The relative change of peak electron density, $(\Delta N_m/N_mF2)$, is computed from the steady-state approximation of RGW equation (7) (with $dN_m/dt = 0$ and no flux), i.e.

$$N_m = 0.8 q_m/\beta_m \tag{7}$$

where q_m and β_m are the production and loss rates at the actual height of the peak. Neutral atmosphere parameters are taken from the MSIS-86 model (Hedin, 1987) and ionospheric rate coefficients are as used by RGW. Since we compute only relative changes of N_mF2, we do not need to specify a value of the solar ionizing flux.

To obtain quantitative estimates of the contributions of specific processes, we define the following scenario for our initial calculations:

(1) The geomagnetic storm is characterized by a sudden commencement at 09:00 L.T. that changes K_p from quiet conditions ($K_p = 1$, $A_p = 4$) to disturbed ($K_p = 7$, $A_p = 132$). We perform the calculations at 15:00 L.T. after 6 h have elapsed with $K_p = 7$. The season is equinox (21 March) for medium solar flux conditions (10.7 cm flux = 120).

(2) Thermospheric parameters are computed from the MSIS model with the time history given in (1) above, i.e. changing from quiet to disturbed conditions ($K_p = 1$–7). This change increases the exospheric temperature T_∞ by about 7% in the longitudes of the dipole tilt, and about 5% elsewhere. There are also changes of chemical composition, which affect the F2-layer. The effects of these changes, at any latitude and longitude, are the "Thermospheric" contributions to the F2-layer storm. It is not practicable in our calculations to separate the effects of thermal expansion and composition changes.

(3) Magnetospheric convection effects are computed using an assumed change in the dawn–dusk electric field from E_{DD} (Quiet) = 0 mV m^{-1} to E_{DD} (Disturbed) = 1.3 mV m^{-1}. Such a pattern simulates the case of no penetration within the plasmasphere, during quiet times, to full penetration during the

initial period of a storm. Carpenter (1970) showed that the magnetospheric electric field near the dusk region is of the order of 0.1 mV m^{-1} under conditions of prolonged quiet, with peak values of 1–4 mV m^{-1} during substorms. Our choice of $E_{DD} = 1.3$ mV m^{-1} conforms to the $K_p = 7$ conditions described by Mendillo and Papagiannis (1971); it represents an appreciable electrodynamic input, though far from the peak values that might be encountered. For a given local time, the latitude variation of the imposed electric field is due only to the geometry of the dipole field, as given by equation (4), and its variation with longitude is due to the tilt of the dipole axis from the rotational axis. The resulting changes are the "Plasma Drift" contributions to the F2-layer storm.

(4) Thermospheric winds with both meridional and zonal components contribute to vertical motions, as given by equation (5). We use a latitude-dependent wind velocity, and the resulting vertical plasma drift W_W varies with longitude because of the tilt of the geomagnetic dipole. The resulting changes are the "Wind" contributions to the F2-layer storm.

Figure 1 gives the meridional and zonal components of the Hedin *et al.* (1988) wind model at 15:00 L.T., averaged over all longitudes for quiet and disturbed conditions. For our initial calculations in Section 3, we consider only the meridional component that plays the dominant role at midlatitudes (though later, in Section 4.5, we include the zonal contribution). To isolate further the "neutral wind" contributions to storm effects, we characterize the quiet pattern ($K_p = 1$) by assuming that the poleward wind decreases linearly from 80 m s^{-1} at $\pm 65°$ latitude to 0 m s^{-1} at the equator, as shown by the straight line in Fig. 1(a). For the disturbed case ($K_p = 7$), we make the simple assumption that the quiet-day poleward winds are exactly cancelled by the opposing pressure gradients due to the storm heating at high latitudes, so that $W_W = 0$ everywhere. This assumption is supported by Fig. 1(a) and by the recent observations by Buonsanto *et al.* (1990) for daytime storm effects at midlatitudes. In the initial set of results that follow, we calculate separately the response of the ionosphere to the three components of the daytime storm, as defined above:

(a) thermospheric effects (due to changes in MSIS from $K_p = 1$ to $K_p = 7$);

(b) plasma drift effects [due to changes from no E

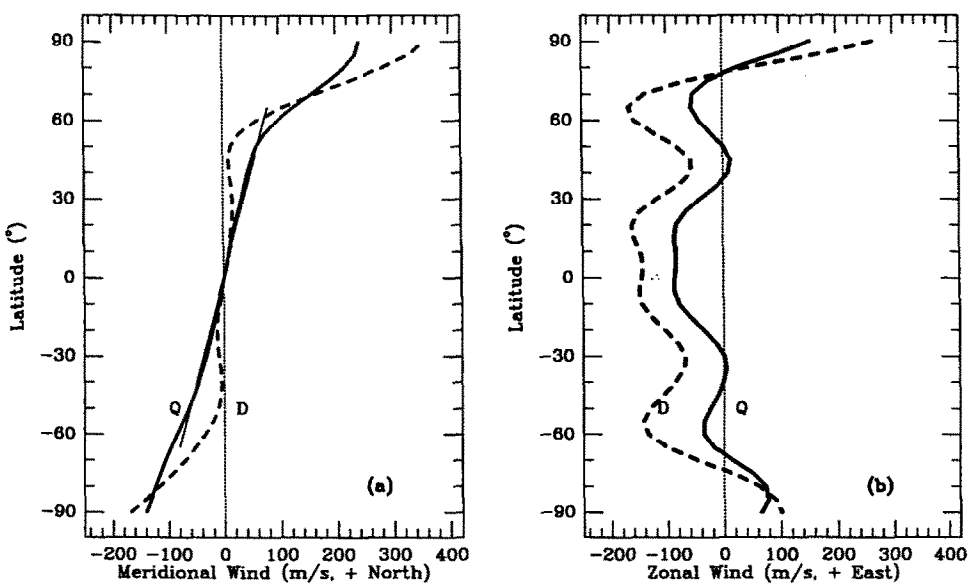

FIG. 1. (a) LONGITUDE-AVERAGED MERIDIONAL WIND (POSITIVE SOUTH TO NORTH) AND (b) LONGITUDE-AVERAGED ZONAL WIND (POSITIVE WEST TO EAST) VS GEOGRAPHIC LATITUDE, FOR 15:00 L.T. AT EQUINOX, SOLAR 10.7 cm flux = 120 units, FROM THE MODEL OF HEDIN *et al.* (1988).
Solid lines refer to quiet magnetic conditions ($K_p = 1$), dashed lines to disturbed conditions ($K_p = 7$). For the purposes of the present paper, the quiet-day meridional wind is represented by the straight-line approximation shown by the thin line, from 65°N to 65°S; the storm-day wind is taken to be zero.

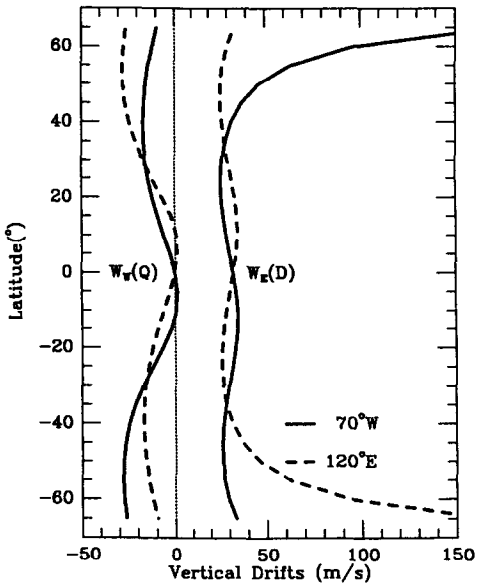

FIG. 2. VERTICAL DRIFT (POSITIVE UPWARDS) VS GEOGRAPHIC LATITUDE AT TWO LONGITUDES, 70°W (SOLID CURVES) AND 120°E (DASHED CURVES).
W_W(Q) is the vertical drift due to the quiet-day poleward wind at $K_p = 1$, corresponding to the straight line in Fig. 1(a); W_E(D) is the vertical plasma drift at $K_p = 7$.

field to a latitude-dependent magnetospheric field as given by equation (4)];

(c) neutral wind effects (due to the cancellation of the quiet-day latitude-dependent wind).

Figure 2 shows the resultant vertical components of the drift due to the quiet-day meridional wind and the storm-day plasma drifts as a function of latitude, at the two extreme longitudes of the tilted dipole field. To illustrate the longitude effects in the vertical drift at fixed latitudes, Fig. 3 shows the wind-produced drift W_W (quiet) and the electromagnetic drift W_E (disturbed) at latitudes of $\pm 65°$, $\pm 45°$ and $\pm 25°$.

3. LONGITUDE VARIATIONS AT FIXED LATITUDES

To illustrate the longitude dependence of ionospheric storm effects associated with the simple storm scenario outlined above, we present in Fig. 4 the changes in h_mF2 that result from thermospheric changes, neutral winds and plasma drifts. Related percentage changes in N_mF2 are given in Fig. 5. To understand the changes induced by each process, we examine the effects at latitudes $\pm 65°$, $\pm 45°$ and $\pm 25°$.

3.1. *Thermospheric effects*

For the case of no winds and no electrodynamic drifts, the values of h_mF2 resulting from the balance height calculations, using MSIS for $K_p = 1$, are given by the squares in Fig. 4 at the chosen latitudes. There is some longitude variation, notably at latitudes $\pm 25°$, where (because of the proximity of the geomagnetic equator) the $\sin^2 I$ factor in the plasma diffusion coefficient is smallest at longitudes around 100°E in the Northern Hemisphere and 70°W in the Southern.

For $K_p = 7$ the balance heights are higher, as shown by the dashed curves in Fig. 4. The differences between the squares and dashed curves are essentially due to thermal expansion which raises the isobaric levels (i.e. the "reduced height" z_mF2 is virtually unchanged by the heating, but the "real height" h_mF2 is increased). The composition changes have a minor effect on h_mF2.

The changes of electron density due to the change of the neutral atmosphere from $K_p = 1$ to $K_p = 7$ are shown by the black dotted curves in Fig. 5. They are computed from equation (7), applied to the actual level of the peak for both quiet and storm conditions. The storm heating effect increases with magnetic latitude, and its longitude variations are thus related to the dipole tilt. At northern midlatitudes, therefore, the negative effect on N_mF2 is greatest in the American sector, while in southern midlatitudes it is greatest in the Indian Ocean sector, i.e. at longitudes closest to the magnetic pole.

As mentioned in Section 2, the "thermospheric" effect includes both thermal expansion and composition changes; the resulting changes in N_mF2, as shown by the black dots in Fig. 5, are mainly attributed to the latter, even though the MSIS model for $K_p = 7$ does not contain the major wind-induced composition changes that characterize the main phase of F2-layer storms.

3.2. *Neutral wind effects*

The addition of the quiet-day neutral wind for $K_p = 1$ [i.e. the linear profile from Fig. 1(a)] results in the change of balance height from the squares to the crosses in Fig. 4. In every case the quiet-day poleward winds reduce h_mF2 at all longitudes. The storm removes this effect, as shown by the transition from crosses to dashed curves in Fig. 4; the dashed curves thus represent h_mF2 with no meridional wind in the $K_p = 7$ thermosphere.

The accompanying changes in electron density are given by the dashed curves in Fig. 5. Removing the meridional wind everywhere increases N_mF2 (all the dashed curves are above the dotted curves), and so tends to offset the negative effect of the thermospheric effect considered in Section 3.1. At lower latitudes

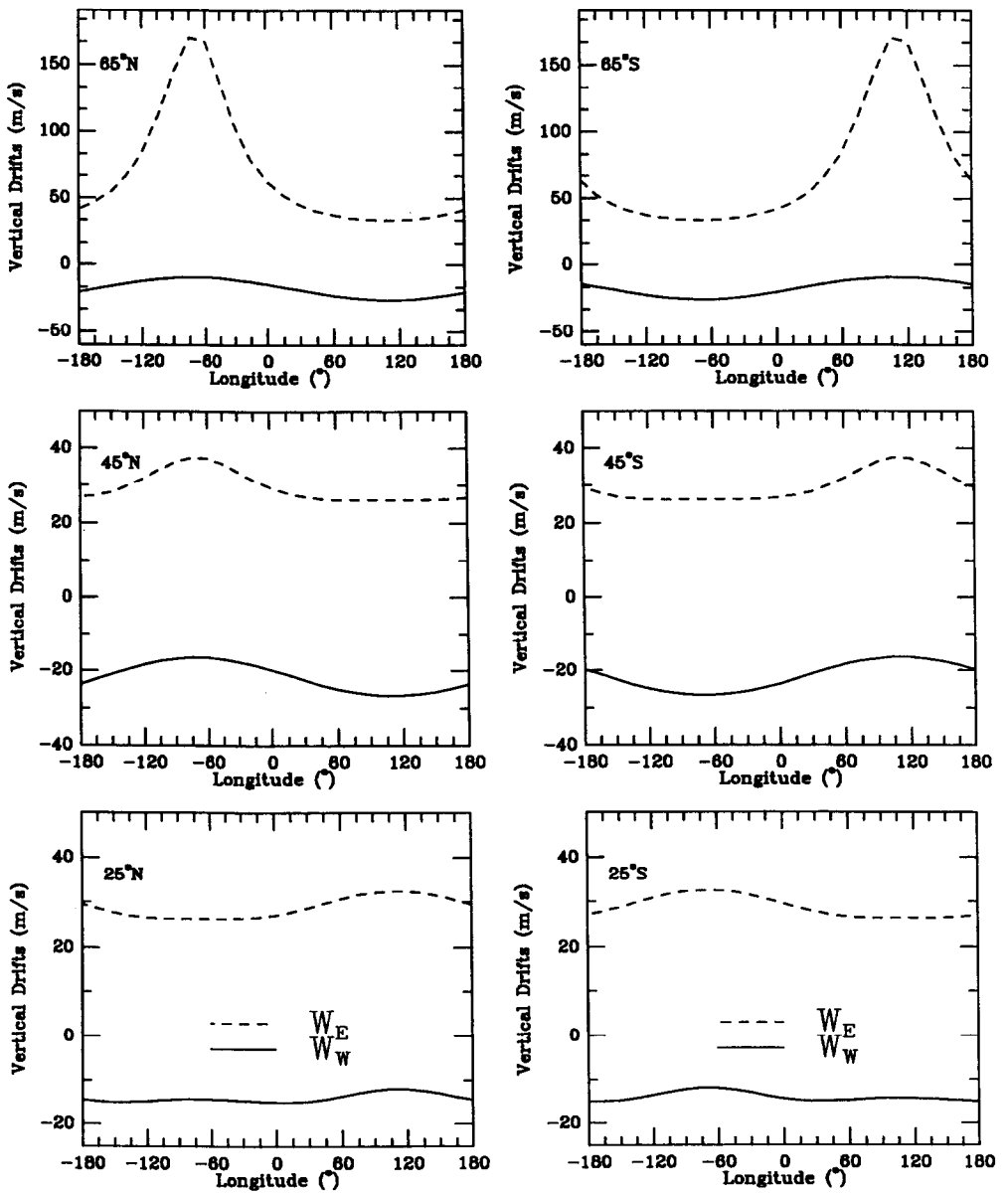

FIG. 3. WIND-PRODUCED DRIFT W_W (QUIET) AND THE ELECTROMAGNETIC PLASMA DRIFT W_E (DISTURBED) VS GEOGRAPHIC LONGITUDE, AT GEOGRAPHIC LATITUDES OF $\pm 65°$, $\pm 45°$ AND $\pm 25°$.

($\pm 25°$), where the thermospheric effect is small, the net effect on N_mF2 is positive, the dashed curves giving $\Delta N_m/N_m > 0$ at all longitudes. However, at $\pm 65°$, the negative "thermospheric" effect is too strong to be offset by the winds (especially at the longitudes of the dipole tilt), and the dashed curves show a net negative effect, with $\Delta N_m/N_m < 0$, except in the South Atlantic sector. Here, because of the relatively small dip angle I, the wind effect is strong enough to give a small net positive effect in N_mF2.

3.3. *Plasma drift effects*

The introduction of the magnetospheric convection field results in the transition from the "static" values

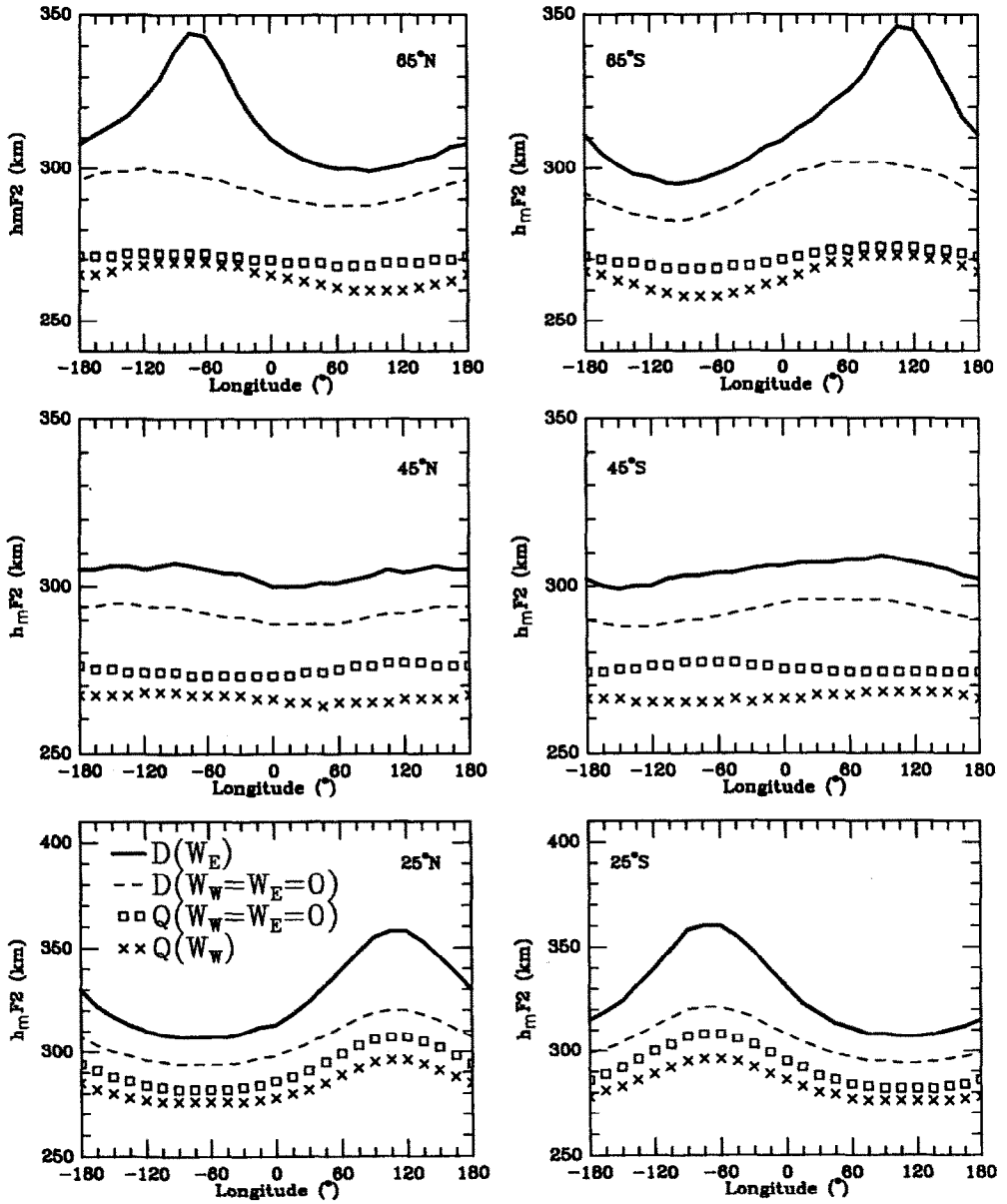

FIG. 4. HEIGHT OF THE F2 PEAK VS LONGITUDE AT LATITUDES 65°, 45° AND 25° IN BOTH HEMISPHERES. For the quiet-day thermosphere ($K_p = 1$), the squares show h_mF2 with no meridional wind and no plasma drift; the crosses show the effect of including the quiet-day meridional wind. For the disturbed thermosphere ($K_p = 7$) with no meridional wind, the dashes and solid lines show h_mF2 with and without plasma drift, respectively.

of h_mF2 (squares in Fig. 4), without winds or drifts, to the solid curve which shows the "storm" electric field effect imposed on the $K_p = 7$ thermosphere. The latitude and longitude dependences of the tilted dipole exert a significant influence on these results. At $\pm 65°$, the large increases of h_mF2 at longitudes 70°W and 120°E are due to the high dipole latitudes, i.e. the predominance of the $\sec^3 \Lambda$ factor in equation (4). At very high dip latitudes (as in the American sector at 65°N and in the South Indian Ocean at 65°S), the drift

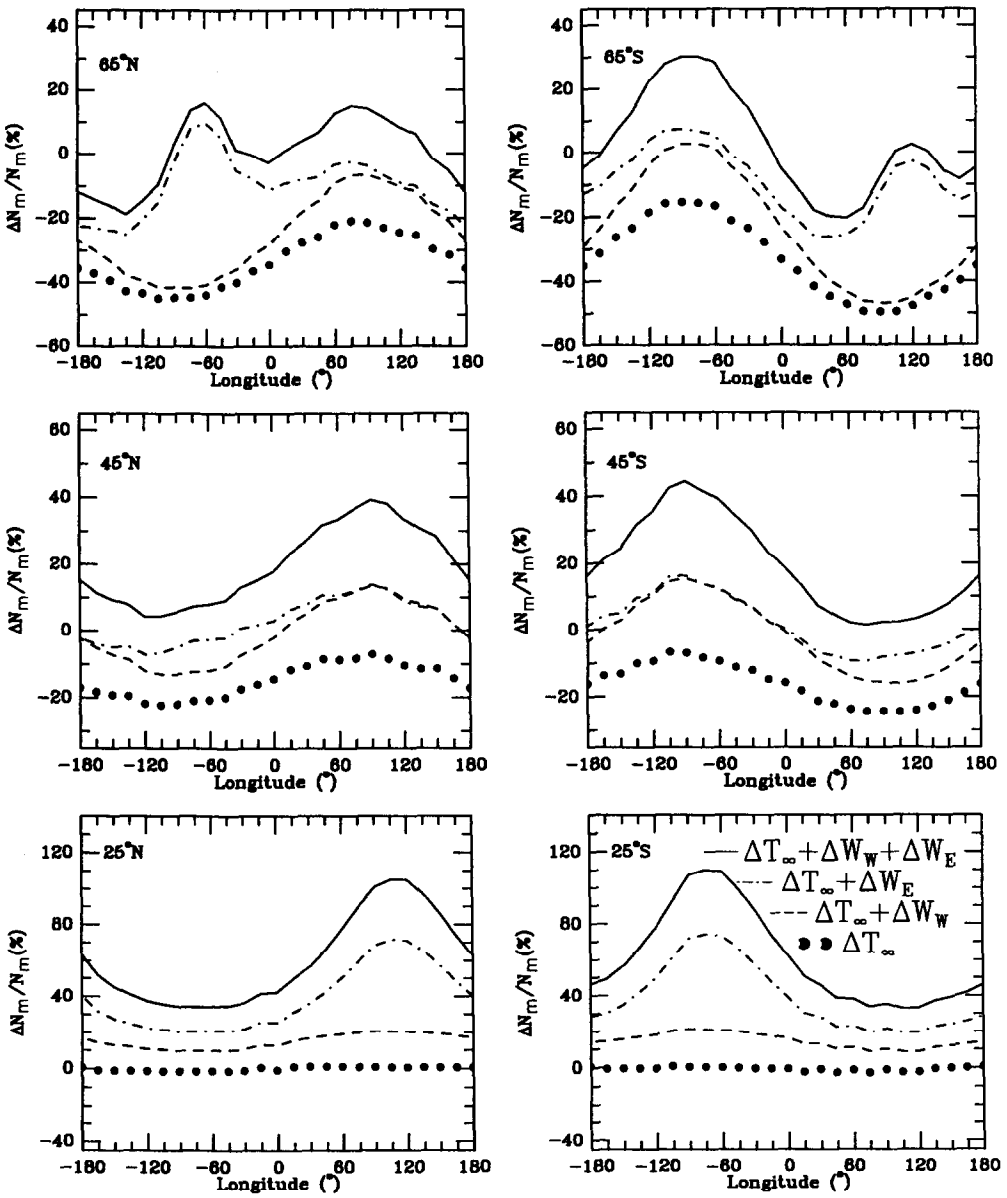

FIG. 5. RELATIVE CHANGES OF PEAK ELECTRON DENSITY, ($\Delta N_m/N_mF2$), VS LONGITUDE AT LATITUDES 65°, 45° AND 25° IN BOTH HEMISPHERES, EXPRESSED AS PERCENTAGES.
The dotted lines show the effect of thermospheric changes only. The dashes show the combined effect of thermospheric changes and of removing the quiet-day meridional wind (as assumed during the storm). The dot–dash curves show the combined effect of thermospheric changes and plasma drift. The solid curves show the combined effect of thermospheric changes, removal of the quiet-day wind and addition of plasma drift.

velocities W_E given by equation (4) may be unrealistically large, but the general form of the results is probably correct.

At latitudes of $\pm 25°$, E/B is smaller than at higher latitudes, but the drift has a larger vertical component because cos I is larger. The effect of the drift on h_mF2 and N_mF2 is largest in the longitudes nearest to the geomagnetic equator, i.e. the East Asian and South American sectors (because of the relatively small dip angle). This situation is the reverse of that at $\pm 65°$.

In considering the effect upon N_mF2, the dominance of the cos I term causes the longitude dependence of the plasma drift effect to be similar to that of the neutral wind effect, at all except the highest latitudes. Figure 5 shows that the plasma drifts counteract the negative "thermospheric" effect, as shown by the dash–dot curves which are mostly above the zero level (at which $\Delta N_m/N_m = 0$), except in those sectors at higher latitudes where the heating is strongest. Furthermore, the positive effects of plasma drift (shown by the difference between the dotted and dash–dot curves) exceed the effect of removing the quiet-day equatorward wind (shown by the difference between the dotted and dashed curves). Plasma drifts are most effective at higher midlatitudes, both at 70°W and 120°E, and give two-humped curves at $\pm 65°$ in Fig. 5. Finally, the solid lines in Fig. 5 show the overall positive patterns that result from all three processes considered.

4. GLOBAL PATTERNS

The results of Section 3 show that even the most simple storm morphologies in ΔT_∞, ΔW_W and ΔW_E result in complex patterns of h_mF2 and $\Delta N_m/N_m$, owing to the geometry of the dipole field. To illustrate the full nature of these patterns, the storm effects portrayed in Figs 3, 4 and 5 were evaluated at 5° intervals in latitudes between $\pm 65°$ and at 15° intervals in longitude to form global maps. As in Section 3, we examine each process separately.

4.1. *Thermospheric effects*

Figure 6 (top left) gives contours of $\Delta N_m/N_m$ that result from thermospheric changes as derived from MSIS for the disturbed versus quiet cases. No winds or plasma drifts are included in the calculations. The latitude and longitude dependences in the daytime storm show the thermospheric effects follow dipole geometry. For example, at geographic latitude 45°N, the ionospheric negative phase is characterized by ΔN_mF2 $\simeq -20\%$ at American longitudes where magnetic latitudes are higher, in comparison to ΔN_mF2 $\simeq -5\%$ in the Asian sector which is at lower magnetic latitudes. While this is not a complete simulation, the results show that thermospheric heating in the auroral zone as portrayed by MSIS is a cause of ionospheric depletions that decrease with latitude. The positive effects at low latitudes are nevertheless consistent with the predominantly positive storm effects observed in the equatorial zone (Matuura, 1972).

4.2. *Neutral wind effects*

To illustrate the nature of the wind effect, we give in Fig. 6 (top right) the pattern of $\Delta N_m/N_m$ that results when MSIS is kept constant (quiet conditions, $K_p = 1$) and the storm wind profile is used (i.e. the cessation of the quiet winds, as illustrated in Fig. 1). The resulting positive effect maximizes at midlatitudes in the American sector in the Southern Hemisphere and the Asian sector in the Northern Hemisphere. As was shown in Fig. 4, the increase of h_mF2 (the difference between the squares and crosses) is greatest at midlatitudes where the sin I cos I cos D terms reach their peak values, especially at the 70°W and 120°E meridians.

4.3. *Plasma drift effects*

To illustrate the nature of the plasma convection effect, we give in Fig. 6 (bottom left) the pattern of $\Delta N_m/N_m$ that results when MSIS is kept constant ($K_p = 1$) and the storm plasma drifts are included. Since electrodynamic processes beyond the plasmapause and within the equatorial zone are far more complex than the simple convection model used here, we omit the plasma drift effects at latitudes above $\pm 65°$ geographic and below $\pm 20°$ magnetic. The resultant pattern shows that the convection fields create a positive phase everywhere, increasing both towards high latitudes [because of the $\sec^3 \Lambda$ factor in equation (4)] and towards the equator (because of the cos I factor). The longitude effects depend on latitude. For example, at latitude 45°S the positive effect is largest in the American sector, while at 30°N it is largest in the Asian sector. Since the thermospheric conditions were held constant for these calculations, they pertain only to the initial hours of a storm.

4.4. *Overall results*

The pattern that emerges when all three processes are included (thermospheric changes, change of wind, plasma convection) is given in Fig. 6 (bottom right). The increases of N_mF2 induced by the changes in neutral winds and electric fields combine to overwhelm the depletions associated with the thermospheric changes. The resultant positive effects on N_mF2 vary significantly with geographic latitude and longitude. In the midlatitude range characterized by 25°–50°, the positive storm effects are greatest near 90°W in the Southern Hemisphere and near 90°E in the Northern Hemisphere. These zones lie to the west of Peru in the South Pacific and in Western China, areas of the globe that are particularly undersampled in terms of F-layer observations.

4.5. *Effects of longitude dependent winds*

The average meridional wind pattern for 15:00 L.T. depicted in Fig. 1(a), together with dipole field geometry, yields the longitude dependences shown in Fig. 6 (top right) and ultimately Fig. 6 (bottom right).

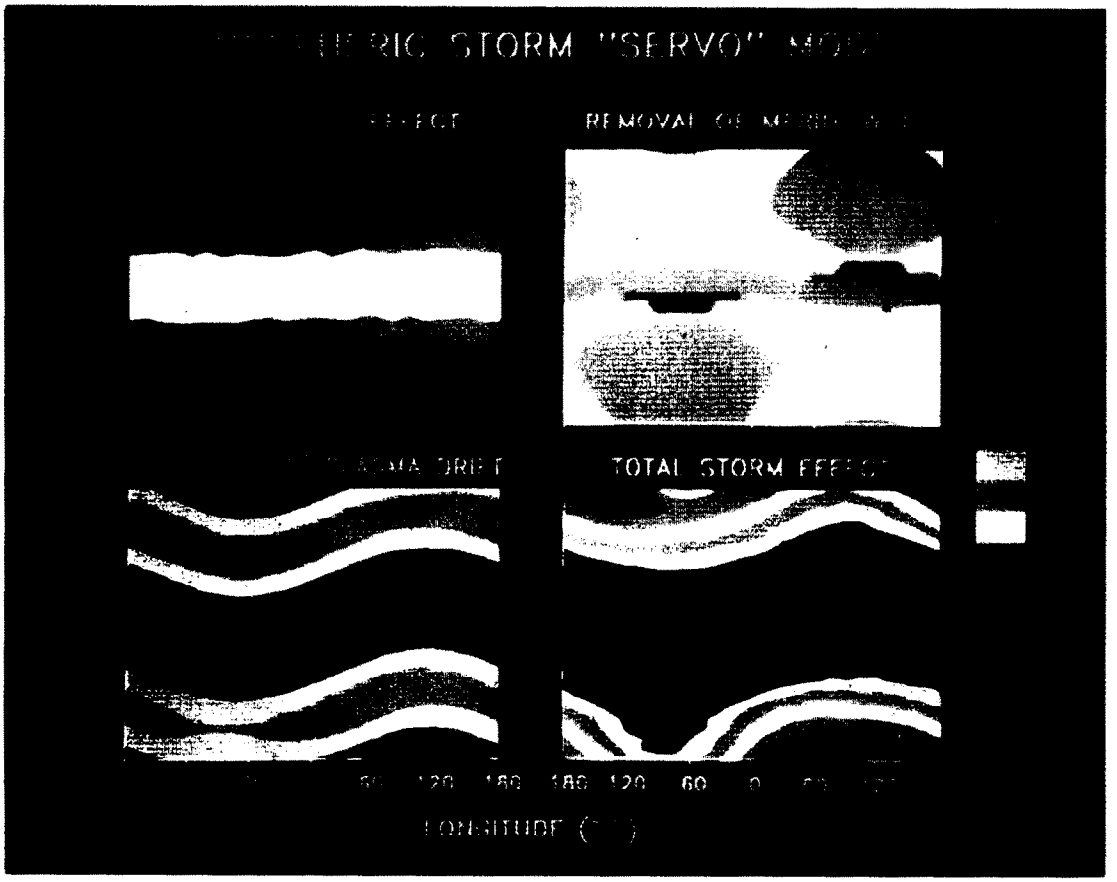

FIG. 6. GLOBAL CONTOURS OF $\Delta N_m/N_m$, THE PERCENTAGE CHANGE IN F2-PEAK ELECTRON DENSITY VS GEOGRAPHIC LATITUDE AND LONGITUDE.

(Top left) Effect of changes in the neutral thermosphere, from $K_p = 1$ to $K_p = 7$. (Top right) Effect of removal of quiet-day neutral wind [see text and Fig. 1(a)], quiet thermosphere with $K_p = 1$. (Bottom left) Effect of plasma drift [given by equation (4)] for quiet thermosphere, $K_p = 1$. (Bottom right) The combined effect of all three perturbations.

However, the wind model of Hedin *et al.* (1988) contains longitude dependences of both meridional and zonal winds. We now investigate the effects of using equation (6) in our "servo model" to give the vertical drift W_w produced by the full Hedin model winds, for both quiet and storm conditions.

The results are shown in Figs 7(a) and 7(b) for the meridional and zonal winds separately, and for both together in Fig. 7(c).

They show considerable differences from those given in Fig. 6 (bottom right) for our simple model with meridional winds only. The main effect is to

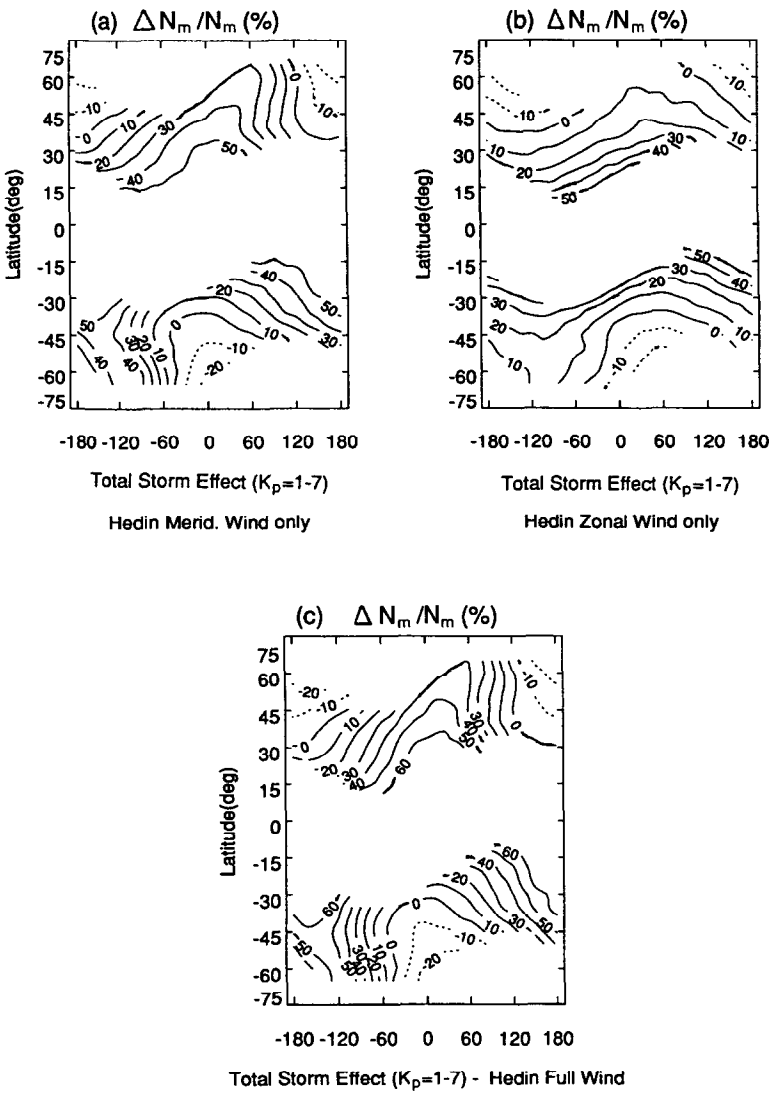

FIG. 7. GLOBAL CONTOURS OF $\Delta N_m/N_m$, THE PERCENTAGE CHANGE IN F2-PEAK ELECTRON DENSITY VS GEOGRAPHIC LATITUDE AND LONGITUDE (SOLID CURVES DENOTE POSITIVE VALUES, DOTTED CURVES DENOTE NEGATIVE VALUES).

(a) The effects of thermospheric changes, Hedin's meridional winds only and plasma drifts are included. (b) The effects of thermospheric changes, Hedin's zonal winds only and plasma drifts are included. (c) The effects of thermospheric changes, Hedin's meridional and zonal winds and plasma drifts are included.

enhance the longitude gradients in the storm perturbations, with some reduction of the latitude gradients, particularly in the longitude sectors of the dipole tilt near 70°W and 120°E.

5. CONCLUSIONS

Storm effects in the midlatitude F2-layer are due to several processes, such as (i) thermal expansion, (ii) changes of neutral gas composition, (iii) equatorward winds and (iv) the penetration of magnetospheric electric fields. Of these, all but (iv) are consequences of the high-latitude heat inputs to the neutral thermosphere and the resulting changes in global thermospheric circulation. In this paper we have examined the effects of all four, though we have included (ii) only to the limited extent portrayed by the empirical MSIS model, and have not been able to separate their effects from those of thermal expansion (i).

We have shown that simple idealized assumptions about winds and fields (as specified in Section 2) give rise to quite complex variations of h_mF2 and N_mF2 with latitude and longitude. Section 3 illustrates the results for fixed latitudes. At $\pm 65°$, the effects of heating and electric fields are strongest in the longitudes to which the geomagnetic dipole is tilted, i.e. the North American and the South Indian Ocean sectors. Because of the proximity of the geomagnetic equator, the situation is reversed at latitudes $\pm 25°$, where the heating and electric field effects are strongest in the East Asian and South American sectors.

In Section 4 we extend the results by showing contour maps of the percentage changes in N_mF2, covering all mid-latitude regions. We note that the maps increase in complexity if we use the full wind model of Hedin *et al.* (1988) (Fig. 7), instead of the simple meridional wind pattern used in Fig. 6.

As MSIS does not fully represent the composition changes produced by the large-scale "storm circulation" in the midlatitude thermosphere (which have a complex morphology in both space and time, and tend to be averaged out in the derivation of MSIS), our calculations do not apply to the "main phase" of F2-layer storms, in which composition effects become dominant. Also important are the travelling ionospheric disturbances that contribute to ionospheric storm effects on time scales of about 1 h (Prölss *et al.*, 1991); they too are excluded from our simulation. Nevertheless, we think our results are of value in illustrating some of the features that can be expected to occur in F2-layer storms, and in showing where these features may be looked for. They may thus have some application to describing and predicting storm effects in the F2-layer.

Acknowledgements—This work was mainly carried out at Boston University, with partial support from NASA contract NAS8-36324. H.R. is most grateful to the Center for Space Physics, Boston University, for hospitality during a sabbatical term. The work at Southampton University was assisted by grant GR/E 73956 from the Science and Engineering Research Council.

REFERENCES

Buonsanto, M. J., Foster, J. C., Galasso, A. D., Sipler, D. P. and Holt, J. M. (1990) Neutral winds and thermosphere/ionosphere coupling and energetics during the geomagnetic disturbances of March 6–10, 1989. *J. geophys. Res.* **95**, 21033.

Carpenter, D. L. (1970) Whistler evidence of the dynamic behavior of the duskside bulge in the plasmasphere. *J. geophys. Res.* **75**, 3837.

Duncan, R. A. (1969) F-region seasonal and magnetic storm behaviour. *J. atmos. terr. Phys.* **31**, 59.

Evans, J. V. (1973) The causes of the storm-time increases of the F-layer at mid-latitudes. *J. atmos. terr. Phys.* **35**, 593.

Fejer, B. G., Spiro, R. W., Wolf, R. A. and Foster, J. C. (1990) Latitudinal variation of perturbation electric fields during magnetically disturbed periods: 1986 SUNDIAL observations and model results. *Ann. Geophys.* **8**, 441.

Hedin, A. E. (1987) MSIS-86 thermospheric model. *J. geophys. Res.* **92**, 4649.

Hedin, A. E., Spencer, N. W. and Killeen, T. L. (1988) Empirical global model of upper thermosphere winds based on *Atmosphere* and *Dynamics Explorer* satellite data. *J. geophys. Res.* **93**, 9959.

Jaggi, R. K. and Wolf, R. A. (1973) Self-consistent calculation of the motion of a sheet of ions in the magnetosphere. *J. geophys. Res.* **78**, 2852.

Lanzerotti, L. J., Cogger, L. L. and Mendillo, M. (1975) Latitude dependence of ionosphere total electron content: observations during sudden commencement storms. *J. geophys. Res.* **80**, 1287.

Matuura, N. (1972) Theoretical models of ionospheric storms. *Space Sci. Rev.* **13**, 124.

Mendillo, M. and Papagiannis, M. (1971) Estimate of the dependence of the magnetospheric electric field on the velocity of the solar wind. *J. geophys. Res.* **76**, 6939.

Prölss, G. W. (1980) Magnetic storm associated perturbations of the upper atmosphere: recent results obtained by satellite-borne gas analyzers. *Rev. Geophys. Space Phys.* **18**, 183.

Prölss, G. W., Brace, L. H., Mayr, H. G., Carignan, G. R., Killeen, T. L. and Klobuchar, J. A. (1991) Ionospheric storm effects at subauroral latitudes: a case study. *J. geophys. Res.* **96**, 1275.

Rishbeth, H. (1972) Thermospheric winds and the F-region: a review. *J. atmos. terr. Phys.* **34**, 1.

Rishbeth, H. (1991) F-region storms and thermospheric dynamics. *J. Geomag. Geoelect.* **43**, in press.

Rishbeth, H., Ganguly, S. and Walker, J. C. G. (1978) Field-aligned and field-perpendicular velocities in the ionospheric F2-layer. *J. atmos. terr. Phys.* **40**, 767.

Southwood, D. J. (1977) The role of hot plasma in magnetospheric convection. *J. geophys. Res.* **82**, 5512.

Spiro, R. W., Wolf, R. A. and Fejer, B. G. (1988) Penetration of high-latitude electric-field effects to low latitudes during SUNDIAL 1984. *Ann. Geophys.* **6**, 39.